

11, 13) or at low temperatures (11, 16). Hence, much of the photodissociated CO cannot escape from the ligand pocket in the 7.5-ns duration of the laser pulse and recombines in a geminate fashion. Further, even for those molecules in which the CO does escape from the ligand pocket, globin relaxation does not proceed fully to completion in the crystal before rebinding of CO occurs.

Our results show that nanosecond time-resolved macromolecular crystallography is indeed feasible and extend the time resolution of macromolecular crystallography by six orders of magnitude, from milliseconds (27) to nanoseconds. The time resolution can be extended to the 100-ps domain if shorter laser pulses are used. Purposeful experimental design and Laue data acquisition and reduction strategies (22, 23) yield significant features in the resultant time-dependent difference electron density maps, even from the weak diffraction patterns resulting from x-ray exposure times of only 150 ps.

#### REFERENCES AND NOTES

1. J.-L. Martin and M. H. Vos, *Annu. Rev. Biophys. Biomol. Struct.* **21**, 199 (1992).
2. D. W. J. Cruickshank, J. R. Helliwell, L. N. Johnson, Eds., *Time-resolved Macromolecular Crystallography* (Oxford Science Publications, Oxford, UK, 1992); K. Moffat, *Annu. Rev. Biophys. Biomol. Struct.* **18**, 309 (1989).
3. J. M. Bolduc *et al.*, *Science* **268**, 1312 (1995).
4. S. Sikora, A. S. Little, T. G. Dewey, *Biochemistry* **33**, 4454 (1994).
5. T.-Y. Teng, V. Šrajcar, K. Moffat, *Nature Struct. Biol.* **1**, 701 (1994). Coordinates from related studies by Schlichting *et al.*, *Nature* **317**, 808 (1994) and Hartmann *et al.*, *Proc. Natl. Acad. Sci. U.S.A.* **93**, 7013 (1996) are not yet available. The three studies differ in key experimental conditions.
6. K. Moffat and R. Henderson, *Curr. Opin. Struct. Biol.* **5**, 656 (1995).
7. K. Moffat, D. Szebenyi, D. Bilderback, *Science* **223**, 1423 (1984).
8. S. Franzen, B. Bohn, C. Poyart, J.-L. Martin, *Biochemistry* **34**, 1224 (1995).
9. S. J. Hagen, J. Hofrichter, W. A. Eaton, *Science* **269**, 959 (1995).
10. M. Lim, T. A. Jackson, P. A. Anfirud, *ibid.*, p. 962; *J. Chem. Phys.* **102**, 4355 (1995).
11. A. Ansari, C. Jones, E. R. Henry, J. Hofrichter, W. A. Eaton, *Biochemistry* **33**, 5128 (1994).
12. M. Lim, T. A. Jackson, P. A. Anfirud, *Proc. Natl. Acad. Sci. U.S.A.* **90**, 5801 (1993).
13. A. Ansari, C. M. Jones, E. R. Henry, J. Hofrichter, W. A. Eaton, *Science* **256**, 1796 (1992).
14. W. D. Tian, J. T. Sage, V. Šrajcar, P. M. Champion, *Phys. Rev. Lett.* **68**, 408 (1992); L. Genberg, L. Richard, G. McLendon, R. J. D. Miller, *Science* **251**, 1051 (1991); X. Xie and J. D. Simon, *Biochemistry* **30**, 3682 (1991).
15. S. M. Janes, G. A. Dalickas, W. A. Eaton, R. M. Hochstrasser, *Biophys. J.* **54**, 545 (1988).
16. R. H. Austin, K. W. Beeson, L. Eisenstein, H. Frauenfelder, I. C. Gunsalus, *Biochemistry* **14**, 5355 (1975).
17. Q. H. Gibson, J. S. Olson, R. E. McKinnie, R. J. Rohlf, *J. Biol. Chem.* **261**, 10228 (1986).
18. P. Li, J. T. Sage, P. M. Champion, *J. Chem. Phys.* **97**, 3214 (1992); R. Lingle Jr. *et al.*, *J. Am. Chem. Soc.* **113**, 3992 (1991).
19. H. Li, R. Elber, J. E. Straub, *J. Biol. Chem.* **268**, 17908 (1993); K. Kuczera, J.-C. Lambry, J.-L. Martin, M. Karplus, *Proc. Natl. Acad. Sci. U.S.A.* **90**,

- 5805 (1993); O. Schaad, H.-X. Zhou, A. Szabo, W. A. Eaton, E. Henry, *ibid.*, p. 9547.
20. R. Elber and M. Karplus, *J. Am. Chem. Soc.* **112**, 9161 (1990).
21. E. R. Henry, W. A. Eaton, R. M. Hochstrasser, *Proc. Natl. Acad. Sci. U.S.A.* **83**, 8982 (1986).
22. Sperm whale met Mb was used to grow crystals in the monoclinic form at pH 6 (28), which were converted to the MbCO form as described (5). Crystals with typical dimensions of 0.4 mm by 0.3 mm by 0.07 mm contained <5% of met Mb. Optical monitoring (29) with relatively weak (50 mW/mm<sup>2</sup>), polarized light at 543 nm was essential to determine the best conditions for crystal photolysis, and to examine both the extent of photolysis just before the actual x-ray data collection and the kinetics of ligand rebinding after photolysis. The crystals were photolyzed by unpolarized 7.5-ns pulses at 635 nm from a Nd:YAG pumped dye laser (Continuum NY61-10/ND60), with DCM 630 dye. At 635 nm the crystal absorbance  $A$  is  $\approx 0.2$ , which ensures relatively uniform photolysis in the longitudinal direction and minimizes photochemical and thermal gradients (30). Absorbance changes  $\Delta A$  of crystals were measured as a function of laser pulse energy density to determine appropriate conditions for maximum photolysis. We estimate that a relative absorbance change,  $\Delta A/A$ , of 0.25 at 543 nm would be observed on complete photolysis. The maximum value of  $\Delta A/A$  before irreversible crystal damage occurred was 0.1 to 0.12, which corresponds to 40 to 50% photolysis, and was accomplished with a pulse energy of 13 mJ and an 0.75-mm diameter laser beam size at the crystal location. Only about 0.5 to 1 mJ of the pulse energy was actually absorbed by the crystals, because of their small cross-sectional area and low absorbance at this wavelength. This corresponds to a photolysis rate of

- about  $10^9$  s<sup>-1</sup>, which in turn is equivalent to about five photons absorbed per pulse per molecule. If we assume that half of the absorbed laser pulse energy appears as heat (16), the maximum temperature jump in the crystal does not exceed 10 K.
23. D. Bourgeois *et al.*, *J. Synchrotron Rad.* **3**, 65 (1996).
24. S. E. V. Phillips, *Brookhaven Protein Data Bank* (1981), Identification Code 1MBD.
25. J. Kuriyan, S. Wilz, M. Karplus, G. A. Petsko, *J. Mol. Biol.* **192**, 133 (1986).
26. L. Zhu, J. T. Sage, A. A. Rigos, D. Morikis, P. M. Champion, *ibid.* **224**, 207 (1992); I. E. T. Iben, L. Keszthelyi, D. Ringe, G. Váró, *Biophys. J.* **56**, 459 (1989); D. Morikis, T. J. Sage, A. K. Rizos, P. M. Champion, *J. Am. Chem. Soc.* **110**, 6341 (1988).
27. U. Genick *et al.*, in preparation.
28. J. C. Kendrew and R. G. Parrish, *Proc. R. Soc. London Ser. A* **238**, 305 (1956).
29. Y. Chen, V. Šrajcar, K. Ng, A. LeGrand, K. Moffat, *Rev. Scient. Instrum.* **65**, 1506 (1994).
30. K. Ng, E. D. Getzoff, K. Moffat, *Biochemistry* **34**, 879 (1995).
31. Z. Ren and K. Moffat, *J. Appl. Cryst.* **28**, 461 (1995); *ibid.*, p. 482.
32. We thank J.-L. Laclare and the accelerator physics staff of ESRF for assistance; M. Roth for the use of his pulsed laser and for assistance and discussions; S. Laboué, C. Rubin, and A. LeGrand for experimental assistance; and C.-I. Brändén for continued support. Supported by the W. M. Keck Foundation, NIH GM 36452 and RR 07707 (K.M.), and a grant-in-aid for Scientific Research on Priority Areas (06235102) from the Ministry of Education, Science, and Culture, Japan (S.-i.A.).

8 July 1996; accepted 15 October 1996

## Survival of Cholinergic Forebrain Neurons in Developing p75<sup>NGFR</sup>-Deficient Mice

Catharina E. E. M. Van der Zee, Gregory M. Ross, Richard J. Riopelle, Theo Hagg\*

The functions of the low-affinity p75 nerve growth factor receptor (p75<sup>NGFR</sup>) in the central nervous system were explored *in vivo*. In normal mice, approximately 25 percent of the cholinergic basal forebrain neurons did not express TrkA and died between postnatal day 6 and 15. This loss did not occur in p75<sup>NGFR</sup>-deficient mice or in normal mice systemically injected with a p75<sup>NGFR</sup>-inhibiting peptide. Control, but not p75<sup>NGFR</sup>-deficient, mice also had fewer cholinergic striatal interneurons. Apparently, p75<sup>NGFR</sup> mediates apoptosis of these developing neurons in the absence of TrkA, and modulation of p75<sup>NGFR</sup> can promote neuronal survival. Cholinergic basal forebrain neurons are involved in learning and memory.

Nerve growth factor (NGF) acts primarily through activation of its specific high-affinity TrkA tyrosine kinase receptor (1, 2). The p75<sup>NGFR</sup> is the product of a different gene and can bind all NGF-related neurotrophins (1, 2). The complete set of p75<sup>NGFR</sup> functions remains to be elucidated, but may include (1, 2) providing ligand-

binding specificity for NGF, enhancement of TrkA function, and mediating retrograde transport of selected neurotrophins (3). The p75<sup>NGFR</sup> has at least two TrkA-independent signaling capacities: by its induction of NF- $\kappa$ B (4) and activation of the sphingomyelin pathway (5). Activation of the sphingomyelin pathway and formation of ceramide (5) can initiate apoptosis (cell death) through the stress-associated protein kinase pathway (6). Ceramide can stimulate cell proliferation, differentiation, and survival (7) perhaps through its metabolite sphingosine-1-phosphate, which activates mitogenic pathways and inhibits ceramide (8). When p75<sup>NGFR</sup> is overexpressed in im-

C. E. E. M. Van der Zee and T. Hagg, Department of Anatomy and Neurobiology, Tupper Building, Dalhousie University, Halifax, Nova Scotia B3H 4H7, Canada. G. M. Ross and R. J. Riopelle, Department of Medicine (Neurology), Queen's University, Kingston, Ontario K7L 2V7, Canada.

\*To whom correspondence should be addressed. E-mail: thagg@is.dal.ca

mortalized neuronal cells (9) or its intracellular domain is overexpressed in transgenic mice (10), neuronal death results. Antisense oligonucleotides against  $p75^{NGFR}$  enhance survival of NGF-deprived differentiated PC12 cells and perinatal sensory neurons (11). However, participation of  $p75^{NGFR}$  in "normal" neuronal death in vivo remains unclear.

Developing cholinergic neurons of the basal forebrain express  $p75^{NGFR}$  and TrkA receptors and respond to NGF (12, 13). We investigated whether these neurons undergo developmental death, and the contribution of  $p75^{NGFR}$ , by comparing control mice with transgenic mice lacking  $p75^{NGFR}$  and with control mice injected with a  $p75^{NGFR}$ -inhibiting peptide. Mice homozygous for a null mutation of  $p75^{NGFR}$  ( $p75^{NGFR}$ -deficient, 129/Sv-derived J1 embryonic stem cell line) (14), the two DNA control strains (129/Sv and Balb/c), and another normal strain (C57Bl/6J/black 29) were obtained from Jackson Laboratory (Maine, USA). Adult (4 to 10 weeks)  $p75^{NGFR}$ -deficient mice had many

more choline acetyltransferase (ChAT)-positive (cholinergic) neurons of the medial septum basal forebrain than did their controls (Fig. 1, A and D). All three control strains showed a 25% reduction in the number of cholinergic neurons between postnatal day 6 and 15 (denoted P6 and P15) to the level observed in adults (Fig. 2A). In  $p75^{NGFR}$ -deficient mice, the number of cholinergic neurons remained the same after P6, and the mice had 50% more cholinergic neurons than did control mice beyond P15 (Fig. 2A). Thus,  $p75^{NGFR}$  appears to be essential for postnatal developmental death of a substantial proportion of the septal cholinergic neurons.

Because loss of ChAT does not indicate cell death (15), we determined whether medial septum neurons undergo the DNA fragmentation characteristic of apoptosis (16). Many apoptotic cells (TUNEL method, Apoptag kit, Oncor, Gaithersburg, Maryland) were visible in control mice during the period of ChAT-positive neuron loss (P4 through P10), but very few apoptotic cells were detected in  $p75^{NGFR}$ -defi-

cient mice (Fig. 2B). On the basis of their distribution, this apoptotic population most likely includes cholinergic neurons. Other septal neurons may also undergo apoptosis, considering the number of detectable apoptotic cells and the limited period in which such cells can be detected (16).

At any age, the number of  $p75^{NGFR}$ -positive medial septum neurons in control mice was the same as the ChAT-positive number. At P6, only ~75% expressed TrkA [analysis of variance (ANOVA)  $P < 0.01$ ]. During the time of neuronal loss (P6 through P15), the number of TrkA-positive

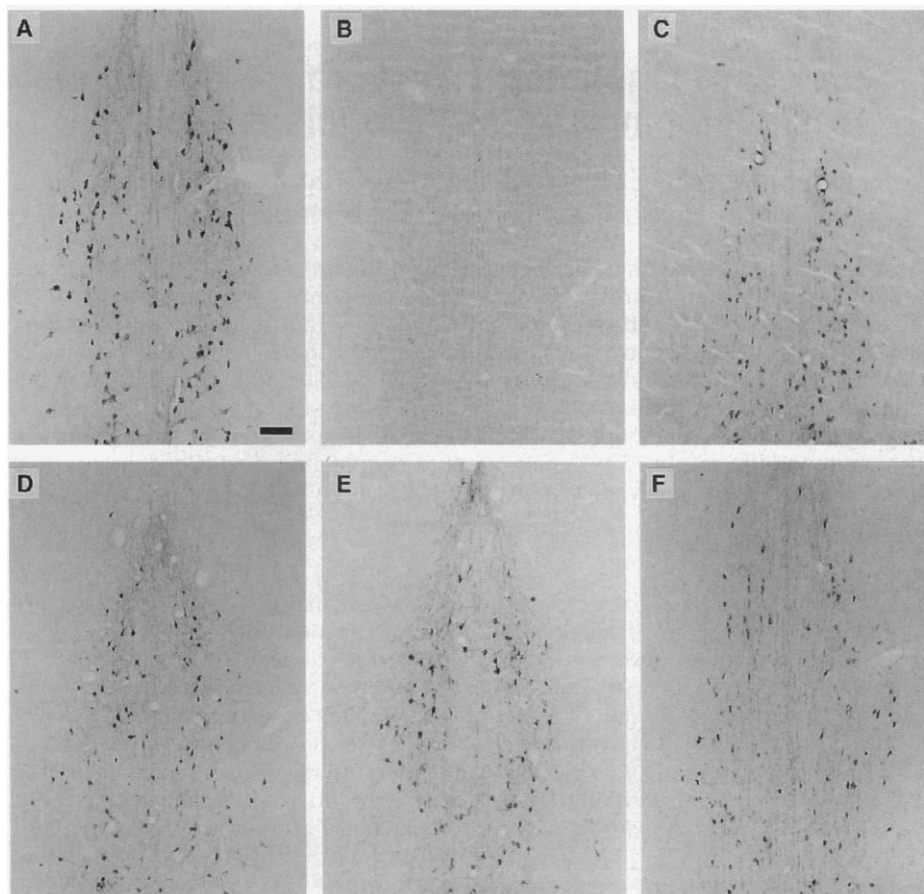


**Fig. 1.** Coronal sections through the medial septum reveal that adult  $p75^{NGFR}$ -deficient mice (**A**) have more cholinergic (ChAT-positive) basal forebrain neurons than do control mice (**D**). Bar, 100  $\mu$ m. The lack of  $p75^{NGFR}$  immunoreactivity in the transgenic mice (**B**) and presence in controls (**E**) confirmed genotype. Similar numbers of TrkA-positive neurons were seen in  $p75^{NGFR}$ -deficient (**C**) and control (**F**) mice. Sections were processed as described (23).

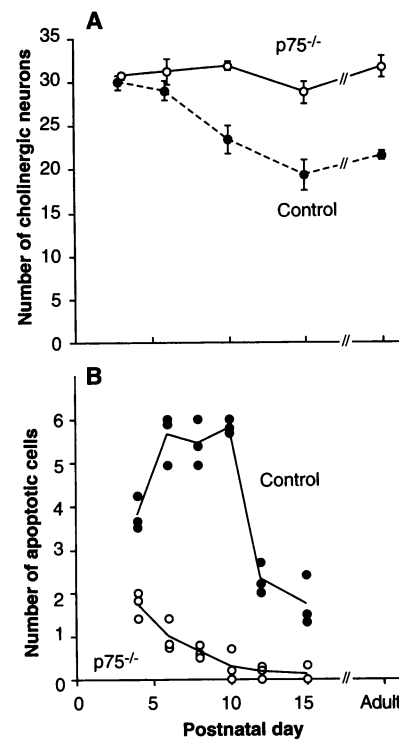


**Fig. 2.** A proportion of postnatal cholinergic neurons in the medial septum undergoes apoptosis in control, but not in  $p75^{NGFR}$ -deficient ( $p75^{-/-}$ ), mice. (**A**) Average number  $\pm$  SEM of ChAT-positive medial septum neurons per 30- $\mu$ m section (six to eight sections per mouse) at different postnatal ages (P0 is the day of birth). In control mice, 25% of the neurons disappeared between P6 and P15 [ $P < 0.0001$ , ANOVA,  $F(4,41) = 15.682$ ]. Adult  $p75^{NGFR}$ -deficient mice ( $n = 14$ ) did not show this decrease. The numbers in the three adult control groups (129/Sv,  $n = 6$ ; Balb/c,  $n = 9$ ; and C57Bl/6J/black 29,  $n = 9$ ) were not significantly different and therefore are grouped. At P3, P6, P10, and P15 for control (129/Sv and Balb/c) mice,  $n = 4, 7, 6,$  and  $5$ ; and for  $p75^{NGFR}$ -deficient mice,  $n = 3, 4, 4,$  and  $6$ , respectively. Sections were processed and analyzed as described (23). (**B**) The average number of apoptotic profiles per 10- $\mu$ m medial septum section of control mice was much higher than in  $p75^{NGFR}$ -deficient mice [ $P < 0.0001$ , ANOVA,  $F(1,24) = 759.392$ ]. Values are from individual mice and derive from a separate set of animals than those in Figs. 2A and 3.

neurons remained constant, suggesting that only the TrkA-negative neurons (~25%), seen at P6, die (Fig. 3). In p75<sup>NGFR</sup>-deficient mice, the number of TrkA-positive neurons was always similar to that in control mice, but the number of TrkA-negative cholinergic neurons remained constant (Fig. 3). Thus, p75<sup>NGFR</sup> apparently mediates apoptosis of cholinergic neurons only in the absence of TrkA, and TrkA counteracts this function of p75<sup>NGFR</sup>.

We investigated whether p75<sup>NGFR</sup> plays a role in the developmental death of other neurons in the brain. Cholinergic interneurons in the neostriatum express p75<sup>NGFR</sup> and TrkA in early development (C. E. E. M. Van der Zee, G. M. Ross, R. J.

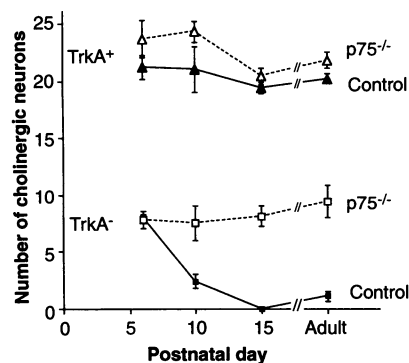


**Fig. 3.** In control mice, apparently only TrkA-negative medial septum neurons disappear between P6 and P15 [ $P < 0.0001$ , ANOVA,  $F(3,23) = 46.549$ ]. The average number  $\pm$  SEM of cholinergic neurons in control and p75<sup>NGFR</sup>-deficient (p75<sup>-/-</sup>) mice was separated into TrkA-positive and TrkA-negative (ChAT-positive minus TrkA-positive) groups. Sections were processed and analyzed as described (23). At P6, P10, P15, and adult ages for control mice (129/Sv and Balb/c),  $n = 6, 6, 3$ , and  $12$ ; and for p75<sup>NGFR</sup>-deficient mice,  $n = 5, 4, 4$ , and  $10$ , respectively.

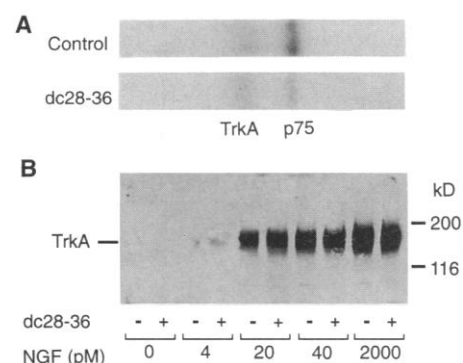


**Fig. 4.** (A) dc28-36 (100  $\mu$ M) reduces <sup>125</sup>I-NGF affinity crosslinking to p75<sup>NGFR</sup> (>50%), but not to TrkA, in PC12 cells, as measured by optical density of autoradiographic signal. (B) dc28-36 (100  $\mu$ M) does not affect NGF-induced TrkA phosphorylation in PC12 cells. Immunoprecipitated and electrophoretically separated TrkA was identified with phosphorylated tyrosine antibodies.

Riopelle, T. Hagg, unpublished results) (12), but only detectable amounts of TrkA during adulthood (12, 17). Adult p75<sup>NGFR</sup>-deficient mice ( $n = 14$ ) had 23% more striatal cholinergic neurons than did controls ( $n = 18$ ;  $53 \pm 2$  neurons compared with  $43 \pm 2$  neurons per  $\text{mm}^2$ ,  $P < 0.001$ ). The number of Purkinje cells in the cerebellum that express p75<sup>NGFR</sup>, but not TrkA, during development and adulthood (17, 18) was the same in adult control and p75<sup>NGFR</sup>-deficient mice ( $304 \pm 7$  cells per 7 mm lobule length for both,  $n = 5$  each). How p75<sup>NGFR</sup> mediates death of neostriatal neurons and not Purkinje cells remains to be resolved.

To further explore the death-inducing role of p75<sup>NGFR</sup>, we designed a p75<sup>NGFR</sup>-interfering peptide (dc28-36) that mimics the p75<sup>NGFR</sup>-binding Loop 1 of NGF (19). Peptide dc28-36 inhibited binding of <sup>125</sup>I-labeled NGF to p75<sup>NGFR</sup> by ~20% in PC12 cells (Table 1) and caused >50% reduction in the <sup>125</sup>I-NGF crosslinking to p75<sup>NGFR</sup>, but not to TrkA (Fig. 4A). In PC12 cells, dc28-36 had no effect on <sup>125</sup>I-NGF binding to TrkA, TrkA-mediated <sup>125</sup>I-NGF uptake, NGF-dependent survival (Table 1), or TrkA phosphorylation (Fig. 4B). Thus, dc28-36 specifically interferes with the p75<sup>NGFR</sup>-NGF interaction in vitro.

**Table 1.** dc28-36 peptide is a specific inhibitor of NGF binding to p75<sup>NGFR</sup>. For design of dc28-36 see (19). All assays were performed as described (22).

NGF (nM)	dc28-36 ( $\mu$ M)	Receptors	Control (%) $\pm$ SEM
<i>Inhibition of steady-state specific binding of <sup>125</sup>I-NGF to p75<sup>NGFR</sup> but not to TrkA in PC12 cells*</i>			
0.5	0	p75 <sup>NGFR</sup> , TrkA	100
0.5	100	p75 <sup>NGFR</sup> , TrkA	87 $\pm$ 4†
0.5	0	TrkA‡	100
0.5	100	TrkA‡	133 $\pm$ 42
<i>Inhibition of <sup>125</sup>I-NGF binding to PC12nhr5 predominantly expressing p75<sup>NGFR</sup></i>			
0.5	0	p75 <sup>NGFR</sup>	100
0.5	2	p75 <sup>NGFR</sup>	102 $\pm$ 6
0.5	50	p75 <sup>NGFR</sup>	83 $\pm$ 3†
0.5	200	p75 <sup>NGFR</sup>	84 $\pm$ 2†
<i>No effect on (TrkA-mediated) <sup>125</sup>I-NGF uptake in PC12 cells</i>			
0.04	0	p75 <sup>NGFR</sup> , TrkA	100§
0.04	200	p75 <sup>NGFR</sup> , TrkA	96 $\pm$ 4
<i>No effect on NGF-dependent survival of PC12 cells  </i>			
0.04	0	p75 <sup>NGFR</sup> , TrkA	100
0.04	200	p75 <sup>NGFR</sup> , TrkA	103 $\pm$ 3

\*Calculated p75<sup>NGFR</sup> occupancy (total-TrkA) at 100  $\mu$ M dc28-36 =  $84 \pm 4\%$ . † $P < 0.01$ , Student's  $t$  test. ‡Brain-derived neurotrophic factor (5 nM) was used to prevent NGF binding to p75<sup>NGFR</sup> but not to TrkA. §100% is 1.25 fmol of NGF per  $10^6$  cells taken up over 30 min at 37°C. ||In serum-free conditions, 48 hours at 37°C.

Mice were injected daily from P0 (P0 is the day of birth) through P15 subcutaneously (the blood-brain barrier is still open at this time) (20) with saline or saline containing dc28-36. At P15, the number of cholinergic medial septum neurons in dc28-36 peptide-treated control mice was ~43% higher than in saline- or noninjected P15 controls (Table 2). Thus, dc28-36 had prevented the death of these neurons, similar to noninjected or dc28-36 peptide-treated p75<sup>NGFR</sup>-deficient mice (Table 2). This provides additional evidence that p75<sup>NGFR</sup> mediates the death of developing cholinergic neurons in vivo.

The mechanisms of p75<sup>NGFR</sup>-induced apoptosis in forebrain cholinergic neurons remain to be resolved. Potentially, binding of ligand (most likely neurotrophins) to p75<sup>NGFR</sup> could induce apoptosis through the TrkA-independent ceramide pathway (5, 6). The observation that TrkA can inhibit ceramide formation (5) is consistent with our finding that all surviving cholinergic neurons expressed TrkA. In the absence of NGF, p75<sup>NGFR</sup> can induce neuronal death by inhibiting ligand-independent TrkA autophosphorylation, that is, prevent the intrinsic survival-promoting signaling of TrkA (1, 11). This mechanism probably does not play a role in the developmental death of the cholinergic basal forebrain neurons, because apparently only those lacking TrkA died. Others have suggested a death-mediating role for unbound p75<sup>NGFR</sup> in the absence of TrkA (9, 21).

The mechanism whereby peptide dc28-36 mimicked the phenotype of the p75<sup>NGFR</sup> null mutation (no basal forebrain neuron loss) in control mice remains to be resolved. In vitro, dc28-36 had a relatively small inhibitory effect on binding but a pro-

**Table 2.** dc28-36 prevents death of developing cholinergic basal forebrain neurons in control mice. Peptide dc28-36 was injected subcutaneously daily from P0 through P15 (29  $\mu$ g/g of body weight; 0.1 ml of 250  $\mu$ M; molecular weight = 1163 daltons). The average number of cholinergic neurons per medial septum section was determined at P15 (23). Control groups contained 129/Sv and Balb/c mice, which had similar neuron numbers.

Treatment group	Number $\pm$ SEM	$n$
Control + none	19.3 $\pm$ 1.8	5
Control + saline	19.4 $\pm$ 1.1	8
Control + dc28-36	27.8 $\pm$ 1.2*	7
p75 <sup>NGFR</sup> -deficient + none	28.6 $\pm$ 1.0*	8
p75 <sup>NGFR</sup> -deficient + dc28-36	26.0 $\pm$ 1.0*	4

\*Significantly different [ $P < 0.0001$ , ANOVA,  $F(4,27) = 15.258$ , and supplemental  $t$  test] from noninjected and saline-injected control groups.

nounced blocking effect on crosslinking of NGF to p75<sup>NGFR</sup>. This suggests that the peptide interfered with post-binding conformational changes of ligand or p75<sup>NGFR</sup> or both, thereby blocking activation of death-related pathways. The suggestion that such post-docking events determine the type of downstream signaling from p75<sup>NGFR</sup> emerges from the finding that, although all neurotrophins can bind to p75<sup>NGFR</sup>, only NGF activates NF- $\kappa$ B through p75<sup>NGFR</sup> in Schwann cells (4).

In conclusion, we present in vivo evidence that p75<sup>NGFR</sup> mediates apoptosis of developing cholinergic basal forebrain and neostriatum neurons, and that pharmacological modulation of p75<sup>NGFR</sup> can promote neuronal survival. These findings are relevant to the observation that cholinergic basal forebrain neurons are involved in learning and memory, and degenerate in Alzheimer's disease.

#### REFERENCES AND NOTES

1. L. A. Greene and D. R. Kaplan, *Curr. Opin. Neurobiol.* **5**, 579 (1995).
2. M. Bothwell, *Annu. Rev. Neurosci.* **18**, 223 (1995); M. V. Chao and B. L. Hempstead, *Trends Neurosci.* **18**, 321 (1995).
3. R. Curtis *et al.*, *Neuron* **14**, 1201 (1995).
4. B. D. Carter *et al.*, *Science* **272**, 542 (1996).
5. R. T. Dobrowsky, M. H. Werner, A. M. Castellino, M. V. Chao, Y. A. Hannun, *ibid.* **265**, 1596 (1994); R. T. Dobrowsky, G. M. Jenkins, Y. A. Hannun, *J. Biol. Chem.* **270**, 22135 (1995).
6. Y. A. Hannun and L. M. Obeid, *Trends Biochem. Sci.* **20**, 73 (1995); M. Verheij *et al.*, *Nature* **380**, 75 (1996).
7. M. V. Chao, *Mol. Cell. Neurosci.* **6**, 91 (1995).
8. O. Cuvillier *et al.*, *Nature* **381**, 800 (1996).
9. S. Rabizadeh *et al.*, *Science* **261**, 345 (1993).
10. P. Barker and F. Miller, personal communication.
11. G. L. Barrett and P. F. Bartlett, *Proc. Natl. Acad. Sci. U.S.A.* **91**, 6501 (1994); G. L. Barrett and A. Georgiou, *J. Neurosci. Res.* **45**, 117 (1996).
12. S. Koh and R. Loy, *J. Neurosci.* **9**, 2999 (1989).
13. Y. Li *et al.*, *ibid.* **15**, 2888 (1995).
14. K. F. Lee *et al.*, *Cell* **69**, 737 (1992).
15. T. Hagg, M. Manthorpe, H. L. Vahlsing, S. Varon, *Exp. Neurol.* **101**, 303 (1988); T. Hagg *et al.*, *Brain Res.* **505**, 29 (1989).
16. Y. Gavrieli, Y. Sherman, S. A. Ben-Sasson, *J. Cell Biol.* **119**, 493 (1992); M. C. Raff *et al.*, *Science* **262**, 695 (1993).
17. S. Koh, G. A. Oyler, G. A. Higgins, *Exp. Neurol.* **106**, 209 (1989); T. Sobreviela *et al.*, *J. Comp. Neurol.* **350**, 587 (1994).
18. B. C. Figueiredo, U. Otten, S. Strauss, B. Volk, D. Maysinger, *Dev. Brain Res.* **72**, 237 (1993).
19. We synthesized a conformationally constrained peptide containing the V1 loop region of NGF, which participates in its binding to p75<sup>NGFR</sup> [C. F. Ibanez *et al.*, *Cell* **69**, 329 (1992)] and affects NGF-mediated neurite outgrowth [F. M. Longo *et al.*, *Cell Regul.* **1**, 189 (1990)], but has not been implicated in a direct TrkA interaction. The linear peptide Cys-Ala-Thr-Asp-Ile-Lys-Gly-Lys-Glu-Cys was synthesized [E. Atherton and R. C. Sheppard, *Solid Phase Peptide Synthesis* (IRL Press, Oxford, 1989)] and purified with high-performance liquid chromatography (HPLC). The sequence and composition was confirmed by sequence analysis and mass spectroscopy. The peptide was cyclized by way of disulfide bonds between the Cys residues to the depsi-cyclic product dc28-36 [K. K. Lee, J. A. Black, R. S. Hodges, in *High Performance Liquid Chromatography of Peptides*

and Proteins, C. T. Mant and R. S. Hodges, Eds. (CRC, Boca Raton, FL, 1991), pp. 389-398] and purified by HPLC. The peptide nature was confirmed by appropriate changes in the HPLC retention time of the peptide and by mass spectroscopy.

20. W. Riseau and H. Wolburg, *Trends Neurosci.* **13**, 174 (1990); Y. Krii, J. Fawcett, K. M. Mearow, E. Pertens, J. Diamond, *Soc. Neurosci. Abstr.* **21**, 1539 (1995).
21. G. Tagliatela, C. J. Hibbert, L. A. Hutton, K. Werrbach-Perez, J. R. Perez-Polo, *J. Neurochem.* **66**, 1826 (1996).
22. S. M. Dostaler *et al.*, *Eur. J. Neurosci.* **8**, 870 (1996).
23. All animal procedures were performed according to the Canadian Council for Animal Care guidelines. Mouse brains were processed for histological analysis as described for rats (15). Every third 30- $\mu$ m coronal section through the medial septum was immunoreacted with polyclonal antibodies to ChAT (AB143, Chemicon, Temecula, CA). The two sets of adjacent sections were stained with polyclonal antibodies to TrkA or p75<sup>NGFR</sup> (antiREX) (L. F. Reichardt, Univ. of California, San Francisco). The number of immunoreactive neurons in one half of the medial septum was counted in all of the six to eight sections per marker for each animal, and expressed as

an average per section. Numbers were corrected according to the formula [M. Abercrombie, *Anat. Rec.* **94**, 239 (1946)]  $N = n \times T / (T + D)$ , where N = total number, n = counted profiles, T = section thickness, and D = longest cell diameter. The size of the neurons in control and p75<sup>NGFR</sup>-deficient mice showed an increase up to P15, followed by a decrease to adult values as is seen in rats [E. Gould, N. J. Woolf, L. L. Butcher, *Brain Res. Bull.* **27**, 767 (1991)], but was similar for both groups at each age.

24. We are grateful for the p75<sup>NGFR</sup> and TrkA antibodies from L. F. Reichardt and the excellent technical support from J. Bunker, M. Netheron, and D. Sadi. We thank N. Tatton for guidance with the Apoptag method, J. Hebb for suggesting the peptide experiment, and E. M. Johnson, Jr. (Washington University, St. Louis, MO) and E. M. Shooter (Stanford University, CA) for their helpful input on the manuscript. Supported by Allelix Biopharmaceuticals, Mississauga, Ontario, Canada, and the Network of Centres of Excellence (Canada) (R.J.R. and T.H.) and a Scholarship from the Medical Research Council of Canada (T.H.).

8 July 1996; accepted 3 October 1996

## DPY-26, a Link Between Dosage Compensation and Meiotic Chromosome Segregation in the Nematode

Jason D. Lieb, Elizabeth E. Capowski, Philip Meneely,\*  
Barbara J. Meyer†

The DPY-26 protein is required in the nematode *Caenorhabditis elegans* for X-chromosome dosage compensation as well as for proper meiotic chromosome segregation. DPY-26 was shown to mediate both processes through its association with chromosomes. In somatic cells, DPY-26 associates specifically with hermaphrodite X chromosomes to reduce their transcript levels. In germ cells, DPY-26 associates with all meiotic chromosomes to mediate its role in chromosome segregation. The X-specific localization of DPY-26 requires two dosage compensation proteins (DPY-27 and DPY-30) and two proteins that coordinately control both sex determination and dosage compensation (SDC-2 and SDC-3).

Many sexually reproducing organisms, including *C. elegans*, rely on a chromosome-counting mechanism for determining their sex. In such organisms the two sexes differ in the dosage of their X chromosomes. These organisms have evolved strategies to compensate for this difference in gene dose and thereby prevent a lethal imbalance in gene products. The dosage compensation mechanisms involve chromosome-wide regulation of gene expression (1). In *C. elegans*, hermaphrodites (XX) reduce the level of transcripts from each of their two X chromosomes to equalize X-chromosome gene expression with that of males (XO)

(2-4). A regulatory gene hierarchy controls dosage compensation in *C. elegans*, and hermaphrodites deficient in these genes die from overexpression of their X-linked genes (5, 6). Dosage compensation is implemented by a protein complex that includes products of at least two genetically defined dosage compensation *dumpy* genes, *dpy-26* and *dpy-27* (7). The *dpy-27* gene product, DPY-27, associates specifically with hermaphrodite X chromosomes and is a member of a highly conserved family of proteins involved in chromosome condensation and segregation (4, 8). These properties suggest that dosage compensation is achieved through changes in X chromosome structure (4).

Here, we present a study of the *dpy-26* gene, whose protein product, DPY-26, not only forms a complex with DPY-27 to achieve dosage compensation, but also functions independently of DPY-27 in meiosis. Unlike *dpy-27* mutations, *dpy-26* mu-

J. D. Lieb and B. J. Meyer, Department of Molecular and Cell Biology, University of California, Berkeley, CA 94720, USA.

E. E. Capowski and P. Meneely, Fred Hutchinson Cancer Research Center, Seattle, WA 98104, USA.

\*Present address: Department of Biology, Haverford College, Haverford, PA 19041, USA.

†To whom correspondence should be addressed.